

Universal Quantum Viscosity in a Unitary Fermi Gas

C. Cao, E. Elliott, J. Joseph, H. Wu, J. Petricka¹, T. Schäfer², and J. E. Thomas*

Physics Department, Duke University, Durham, North Carolina 27708

¹Physics Department, Gustavus Adolphus College, Saint Peter, Minnesota 56082

²Physics Department, North Carolina State University, Raleigh, North Carolina 27695

*To whom correspondence should be addressed; E-mail: jet@phy.duke.edu.

A Fermi gas of atoms with resonant interactions is predicted to obey universal hydrodynamics, where the shear viscosity and other transport coefficients are universal functions of the density and temperature. At low temperatures, the viscosity has a universal quantum scale $\hbar n$ where n is the density, while at high temperatures the natural scale is p_T^3/\hbar^2 where p_T is the thermal momentum. We employ breathing mode damping to measure the shear viscosity at low temperature. At high temperature T , we employ anisotropic expansion of the cloud to find the viscosity, which exhibits precise $T^{3/2}$ scaling. In both experiments, universal hydrodynamic equations including friction and heating are used to extract the viscosity. We estimate the ratio of the shear viscosity to the entropy density and compare to that of a perfect fluid.

Ultracold strongly interacting Fermi gases are of broad interest, as they provide a tunable tabletop paradigm for strongly interacting systems, ranging from high temperature supercon-

ductors to nuclear matter. First observed in 2002, quantum degenerate, strongly interacting Fermi gases are being widely studied (1, 2, 3, 4). To obtain strong interactions (characterized by a divergent s-wave scattering length), a bias magnetic field is used to tune the gas to a broad collisional (Feshbach) resonance, where the range of the collision potential is small compared to the interparticle spacing. In this so-called unitary regime, the properties of the gas are universal functions of the density n and temperature T . The universal behavior of the equilibrium thermodynamic properties has been studied in detail (5, 6, 7, 8, 9, 10, 11), whereas the measurement of universal transport coefficients presents new challenges.

The measurement of the viscosity is of particular interest in the context of a recent conjecture, derived using string theory methods, which defines a perfect normal fluid (12). An example of a nearly perfect fluid is the quark-gluon plasma produced in gold ion collisions, which exhibits almost perfect frictionless flow and is thought to be a good approximation to the state of matter that existed microseconds after the Big Bang (13). The conjecture states that the ratio of the shear viscosity η to the entropy density s has a universal minimum, $\eta/s \geq \hbar/(4\pi k_B)$. This ratio is experimentally accessible in a trapped unitary Fermi gas, where the entropy has been measured both globally (6, 9) and locally (10, 11) and the viscosity can be determined from hydrodynamic experiments (14, 15, 16, 17), so that the predicted minimum ratio can be directly compared to that from Fermi gas experiments (16, 17).

In a Fermi gas, the η/s ratio for the normal fluid is expected to reach a minimum just above the superfluid transition temperature (16). This can be understood using dimensional analysis. Shear viscosity has units of momentum/area. For a unitary gas, the natural momentum is the relative momentum $\hbar k$ of a colliding pair of particles, whereas the natural area is the resonant s-wave collision cross section (18), $4\pi/k^2$. Thus, $\eta \propto \hbar k^3$. At temperatures well below the Fermi temperature at which degeneracy occurs, the Fermi momentum sets the scale so $k \simeq 1/L$, where L is the interparticle spacing. Then $\eta \propto \hbar/L^3$ and $\eta \propto \hbar n$. For a normal fluid above the

critical temperature, the scale of entropy density $s \simeq n k_B$, so $\eta/s \simeq \hbar/k_B$. For much higher temperatures above the Fermi temperature, one expects that $\hbar k$ is comparable to the thermal momentum $p_T = \sqrt{2mk_B T}$, giving the scale $\eta \propto p_T^3/\hbar^2 \propto T^{3/2}/\hbar^2$.

To properly measure the shear viscosity with high precision over a wide temperature range, we use universal hydrodynamic equations, which contain both the friction force and the heating rate, to extract the viscosity from two experiments, one for each of two temperature ranges. For measurement at high temperatures, we observe the expansion dynamics of a unitary Fermi gas after release from a deep optical trap and demonstrate the predicted universal $T^{3/2}$ temperature scaling. For measurement at low temperatures, we employ the damping rate of the radial breathing mode, using the raw cloud profiles from our previous work (19). The smooth joining(discontinuity) of the data from the two measurement methods when heating is included(excluded) (20), demonstrates the importance of including the heating as well as the friction force in the universal hydrodynamic analysis.

The experiments employ a 50-50 mixture of the two lowest hyperfine states of ${}^6\text{Li}$, which is magnetically tuned to a broad Feshbach resonance and cooled by evaporation in the optical trap. The initial energy per particle E is measured from the trapped cloud profile (20).

In the high temperature regime, the total energy of the gas E is larger than $2 E_F$, well above the critical energy $E_c < 0.8 E_F$ for the superfluid transition (9, 10, 11). In this case, the density profile is well fit by a Gaussian, $n(x, y, z, t) = n_0(t) \exp(-x^2/\sigma_x^2 - y^2/\sigma_y^2 - z^2/\sigma_z^2)$, where $\sigma_i(t)$ is a time dependent width and $n_0(t) = N/(\pi^{3/2}\sigma_x\sigma_y\sigma_z)$ is the central density and N is the total number of atoms.

The aspect ratio $\sigma_x(t)/\sigma_z(t)$ is measured as a function of time after release to characterize the hydrodynamics, for different energies E between $2.3 E_F$ and $4.6 E_F$, Fig. 1. We also take expansion data at one low energy point $E = 0.6 E_F$, where the viscosity is small compared to that obtained at higher temperatures and the density profile is approximately a zero temperature

Thomas-Fermi distribution. The black curve shows the fit for zero viscosity and no free parameters. To obtain a high signal to background ratio, we measure the aspect ratio only up to 1.4. For comparison, the green dashed curve shows the prediction for a ballistic gas.

We determine the shear viscosity η by using a hydrodynamic description of the velocity field $\mathbf{v}(\mathbf{x}, t)$ in terms of the scalar pressure and the shear viscosity pressure tensor,

$$m (\partial_t + \mathbf{v} \cdot \nabla) v_i = f_i + \sum_j \frac{\partial_j (\eta \sigma_{ij})}{n}, \quad (1)$$

where $\mathbf{f} = -\nabla P/n$ is the force per particle arising from the scalar pressure P and m is the atom mass. For a unitary gas, the bulk viscosity is predicted to vanish in the normal fluid (21, 22), so we do not include it in the analysis for the expansion. The second term on the right describes the friction forces arising from the shear viscosity, where $\sigma_{ij} = \partial v_i / \partial x_j + \partial v_j / \partial x_i - 2\delta_{ij} \nabla \cdot \mathbf{v} / 3$ is symmetric and traceless.

For a unitary gas, the evolution equation for the pressure takes a simple form, since $P = 2\mathcal{E}/3$ (23, 24), where \mathcal{E} is the local energy density (sum of the kinetic and interaction energy). Then, energy conservation and Eq. 1 implies $(\partial_t + \mathbf{v} \cdot \nabla + 5\nabla \cdot \mathbf{v}/3)P = 2\dot{q}/3$. Here, the heating rate per unit volume $\dot{q} = \eta \sigma_{ij}^2/2$ arises from friction due to the relative motion of neighboring volume elements. To express this in terms of the force per particle, f_i , we differentiate this equation for P with respect to x_i , and use the continuity equation for the density to obtain

$$\left(\partial_t + \mathbf{v} \cdot \nabla + \frac{2}{3} \nabla \cdot \mathbf{v} \right) f_i + \sum_j (\partial_i v_j) f_j - \frac{5}{3} (\partial_i \nabla \cdot \mathbf{v}) \frac{P}{n} = -\frac{2}{3} \frac{\partial_i \dot{q}}{n}. \quad (2)$$

Force balance in the trapping potential $U_{trap}(\mathbf{x})$, just before release of the cloud, determines the initial condition $f_i(0) = \partial_i U_{trap}(\mathbf{x})$.

These hydrodynamic equations include both the force and the heating arising from viscosity. The solution is greatly simplified when the cloud is released from a deep, nearly harmonic trapping potential U_{trap} , as $f_i(0)$ is then linear in the spatial coordinate. If we neglect viscosity,

the force per particle and hence the velocity field remain linear functions of the spatial coordinates as the cloud expands. Thus $\partial_i(\nabla \cdot \mathbf{v}) = 0$ and the pressure P does not appear in Eq. 2. By numerical integration (25), we find that non-linearities in the velocity field are very small even if the viscosity is not zero, because dissipative forces tend to restore a linear flow profile. Hence, the evolution equations 1 and 2, are only weakly dependent on the precise initial spatial profile of P and independent of the detailed thermodynamic properties.

We therefore assume that the velocity field is exactly linear in the spatial coordinates. We take $f_i = a_i(t)x_i$ and $\sigma_i(t) = b_i(t)\sigma_i(0)$, i.e., the density changes by a scale transformation (26), where current conservation then requires $v_i = x_i \dot{b}_i(t)/b_i(t)$.

In general, the viscosity takes the universal form $\eta = \alpha(\theta) \hbar n$, where θ is the local reduced temperature and $\eta \rightarrow 0$ in the low density region of the cloud (27, 20). Using the measured trap frequencies, and eqs. 1 and 2, the aspect ratio data are fit to determine the trap averaged viscosity parameter, $\bar{\alpha} = (1/N\hbar) \int d^3\mathbf{x} \eta(\mathbf{x}, t)$, which arises naturally, independent of the spatial profile of η . Since θ has a zero convective derivative everywhere (in the zeroth order adiabatic approximation) and the number of atoms in a volume element is conserved along a stream tube, $\bar{\alpha}$ is a constant that can be compared to predictions for the trapped cloud before release.

As shown in Fig. 1, the expansion data are very well fit over the range of energies studied, using $\bar{\alpha}$ as the only free parameter. We find that the friction force produces a curvature that matches the aspect ratio versus time data, while the indirect effect of heating is significant in increasing the outward force, which increases the fitted $\bar{\alpha}$ by a factor of $\simeq 2$, compared to that obtained when heating is omitted (20).

For measurements at low temperatures, where the viscosity is small, we determine $\bar{\alpha}$ from the damping rate of the radial breathing mode (19). For the breathing mode, the cloud radii change by a scale transformation of the form $b_i = 1 + \epsilon_i$, with $\epsilon_i \ll 1$, and the heating rate in eq. 2 is $\propto \dot{\epsilon}_i^2$, which is negligible. Hence, the force per particle evolves adiabatically. Adding

the trapping force to eq. 1, one obtains the damping rate $1/\tau = \hbar\bar{\alpha}/(3m\langle x^2 \rangle)$ (20, 28).

The fitted viscosity coefficients $\bar{\alpha}$ for the entire energy range are shown in Fig. 2, which can be used to test predictions (29, 30, 31). Despite the large values of $\bar{\alpha}$ at the higher energies, the viscosity causes only a moderate perturbation to the adiabatic expansion, as shown by the expansion data and the fits in Fig. 1. The breathing mode data and expansion data smoothly join, provided that the heating rate is included in the analysis. In contrast, omitting the heating rate produces a discontinuity between the high and low temperature viscosity data (20). The agreement between these very different measurements when heating is included shows that hydrodynamics in the universal regime is well described by eqs. 1 and 2.

To test the prediction of the $T^{3/2}$ temperature scaling in the high temperature regime, we assume that η relaxes to the equilibrium value in the center of the trap, but vanishes in the low density region so that $\bar{\alpha}$ is well defined. This behavior is predicted by kinetic theory (27). We expect that $\bar{\alpha} \simeq \alpha_0$ where $\eta_0 = \alpha_0 \hbar n_0$ is the viscosity at the trap center before release. At high temperatures (15),

$$\alpha_0 = \alpha_{3/2} \theta_0^{3/2}, \quad (3)$$

where $\alpha_{3/2}$ is a universal coefficient. As θ has a zero convective derivative everywhere (in the zeroth order adiabatic approximation), θ_0 at the trap center has a zero time derivative and α_0 is therefore constant as is $\bar{\alpha}$.

The inset in Fig. 2 shows the high temperature (expansion) data for $\bar{\alpha}$ versus the initial reduced temperature at the trap center, θ_0 . Here, $\theta_0 = T_0/T_F(n_0) = (T_0/T_{FI})(n_I/n_0)^{2/3}$. The local Fermi temperature $T_F(n_0) = \hbar^2(3\pi^2 n_0)^{2/3}/(2mk_B)$ and $T_{FI} = E_F/k_B = T_F(n_I)$ is the ideal gas Fermi temperature at the trap center. n_I is the ideal gas central density for a zero temperature Thomas-Fermi distribution. We use $(n_I/n_0)^{2/3} = 4(\sigma_z^2/\sigma_{Fz}^2)/\pi^{1/3}$ and obtain the initial T_0/T_{FI} from the cloud profile (20).

The excellent fit of Eq. 3 to the data, inset Fig. 2, demonstrates that at high temperature, the

viscosity coefficient very well obeys the $\theta_0^{3/2}$ scaling, in agreement with predictions (15). We note that Eq. 3 predicts that α_0 scales nearly as E^3 , because $\theta_0 \propto T_0/n_0^{2/3} \propto E^2$. This explains the factor of $\simeq 10$ increase in the viscosity coefficients as the initial energy is increased from $E = 2.3 E_F$ to $E = 4.6 E_F$.

A precise comparison between the viscosity data and theory requires calculation of the trap-average $\bar{\alpha}$ from the local shear viscosity, where the relation is tightly constrained by the observed $T^{3/2}$ scaling. Our simple approximation $\bar{\alpha} \simeq \alpha_0$, yields $\alpha_{3/2} = 3.4(0.03)$, where 0.03 is the statistical error from the fit. A better estimate based on a relaxation model (32) shows that $\bar{\alpha} = 1.3 \alpha_0$ at high T , yielding $\alpha_{3/2} = 2.6$. At sufficiently high temperature, the mean free path becomes longer than the interparticle spacing, since the unitary collision cross section decreases with increasing energy. In this limit, a two-body Boltzmann equation description of the viscosity is valid. For a Fermi gas in a 50-50 mixture of two spin states, a variational calculation (15) yields $\alpha_{3/2} = 45 \pi^{3/2}/(64\sqrt{2}) = 2.77$, in reasonable agreement with the fitted values.

Finally, Fig. 3 shows an estimate of the ratio of $\eta/s = \alpha \hbar n/s = (\hbar/k_B)\alpha/(s/nk_B) \simeq (\hbar/k_B)\bar{\alpha}/S$, where S is the average entropy per particle of the trapped gas in units of k_B . We obtain S in the low temperature regime from Ref. (9), which joins smoothly to the second virial coefficient approximation for S in the high temperature regime (20). The inset shows the low temperature behavior, which is about five times the string theory limit (red dashed line) near the critical energy (9) $E_c/E_F = 0.7 - 0.8$ (20). We note also that the apparent decrease of the η/s ratio as the energy approaches the ground state (9) $0.48 E_F$ does not require that the local ratio $\rightarrow 0$ as $T \rightarrow 0$, since contributions from the cloud edges significantly increase S compared to the local s at the center.

References and Notes

1. K. M. O'Hara, S. L. Hemmer, M. E. Gehm, S. R. Granade, J. E. Thomas, *Science* **298**, 2179 (2002).
2. S. Giorgini, L. P. Pitaevskii, S. Stringari, *Rev. Mod. Phys.* **80**, 1215 (2008).
3. I. Bloch, J. Dalibard, W. Zwerger, *Rev. Mod. Phys.* **80**, 885 (2008).
4. W. Ketterle, M. W. Zwierlein, *Making, probing and understanding ultracold Fermi gases* (IOS Press, Amsterdam, 2008). In *Ultracold Fermi Gases*, Proceedings of the International School of Physics Enrico Fermi, Course CLXIV, Varenna, 20 - 30 June 2006.
5. J. Kinast, *et al.*, *Science* **307**, 1296 (2005).
6. L. Luo, B. Clancy, J. Joseph, J. Kinast, J. E. Thomas, *Phys. Rev. Lett.* **98**, 080402 (2007).
7. J. T. Stewart, J. P. Gaebler, C. A. Regal, D. S. Jin, *Phys. Rev. Lett.* (2006).
8. H. Hu, P. D. Drummond, X.-J. Liu, *Nature Physics* **3**, 469 (2007).
9. L. Luo, J. E. Thomas, *J. Low Temp. Phys.* **154**, 1 (2009).
10. M. Horikoshi, S. Najajima, M. Ueda, T. Mukaiyama, *Science* **327**, 442 (2010).
11. S. Nascimbène, N. Navon, K. J. Jiang, F. Chevy, C. Salomon, *Nature* **463**, 1057 (2010).
12. P. K. Kovtun, D. T. Son, A. O. Starinets, *Phys. Rev. Lett.* **94**, 111601 (2005).
13. L. P. Csernai, J. I. Kupusta, L. D. McLerran, *Phys. Rev. Lett.* **97**, 152303 (2006).
14. B. A. Gelman, E. V. Shuryak, I. Zahed, *Phys. Rev. A* **72**, 043601 (2005).
15. G. M. Bruun, H. Smith, *Phys. Rev. A* **75**, 043612 (2007).

16. T. Schäfer, *Phys. Rev. A* **76**, 063618 (2007).
17. A. Turlapov, *et al.*, *J. Low Temp. Phys.* **150**, 567 (2008).
18. The experiments are performed far from p-wave Feshbach resonances. The relevant threshold energy for p-wave scattering is then comparable to the barrier height. Using the known C_6 coefficients, the barrier height for ^{40}K is $280 \mu\text{K}$, while for ^6Li , it is 8 mK . Hence, for temperatures in the μK range, as used in the experiments, p-wave scattering is negligible and s-wave scattering dominates.
19. J. Kinast, A. Turlapov, J. E. Thomas, *Phys. Rev. Lett.* **94**, 170404 (2005).
20. Materials and methods are available as supporting material on *Science* online.
21. D. T. Son, *Phys. Rev. Lett.* **98**, 020604 (2007).
22. M. A. Escobedo, M. Mannarelli, C. Manuel, Bulk viscosities for cold Fermi superfluids close to the unitary limit. [Http://arxiv.org/abs/0904.3023v2](http://arxiv.org/abs/0904.3023v2).
23. T.-L. Ho, *Phys. Rev. Lett.* **92**, 090402 (2004).
24. J. E. Thomas, J. Kinast, A. Turlapov, *Phys. Rev. Lett.* **95**, 120402 (2005).
25. T. Schäfer, Dissipative fluid dynamics for the dilute Fermi gas at unitarity: Free expansion and rotation. [Http://arxiv.org/abs/1008.3876v1](http://arxiv.org/abs/1008.3876v1).
26. C. Menotti, P. Pedri, S. Stringari, *Phys. Rev. Lett.* **89**, 250402 (2002).
27. P. Massignan, G. M. Bruun, H. Smith, *Phys. Rev. A* **71**, 033607 (2005).
28. We give the damping rate $1/\tau$ for a cylindrically symmetric cigar-shaped trap. For $\delta \equiv (\omega_x - \omega_y)/\sqrt{\omega_x\omega_y} \ll 1$, with ω_x, ω_y the transverse trap frequencies, $1/\tau$ contains an additional factor $1 - \delta$.

29. H. Guo, D. Wulin, C.-C. Chien, K. Levin, Microscopic approach to viscosities in superfluid Fermi gases: From BCS to BEC. [Http://arxiv.org/abs/1008.0423v3](http://arxiv.org/abs/1008.0423v3).
30. E. Taylor, M. Randeria, *Phys. Rev. A* **81** (2010).
31. T. Enss, R. Haussmann, W. Zwerger, Viscosity and scale invariance in the unitary Fermi gas. [Http://dx.doi.org/10.1016/j.aop.2010.10.002](http://dx.doi.org/10.1016/j.aop.2010.10.002).
32. T. Schäfer, C. Chafin, Scaling flows and dissipation in the dilute Fermi gas at unitarity. [Http://arxiv.org/abs/0912.4236v3](http://arxiv.org/abs/0912.4236v3).
33. This research is supported by the Physics Divisions of the National Science Foundation, the Army Research Office, the Air Force Office Office of Sponsored Research, and the Division of Materials Science and Engineering, the Office of Basic Energy Sciences, Office of Science, U.S. Department of Energy. T. S. and J. E. T. are affiliated with the ExtreMe Matter Institute (EMMI).

Supporting Online Material

www.sciencemag.org

Materials and Methods

Fig. S1, S2

Supporting References and Notes

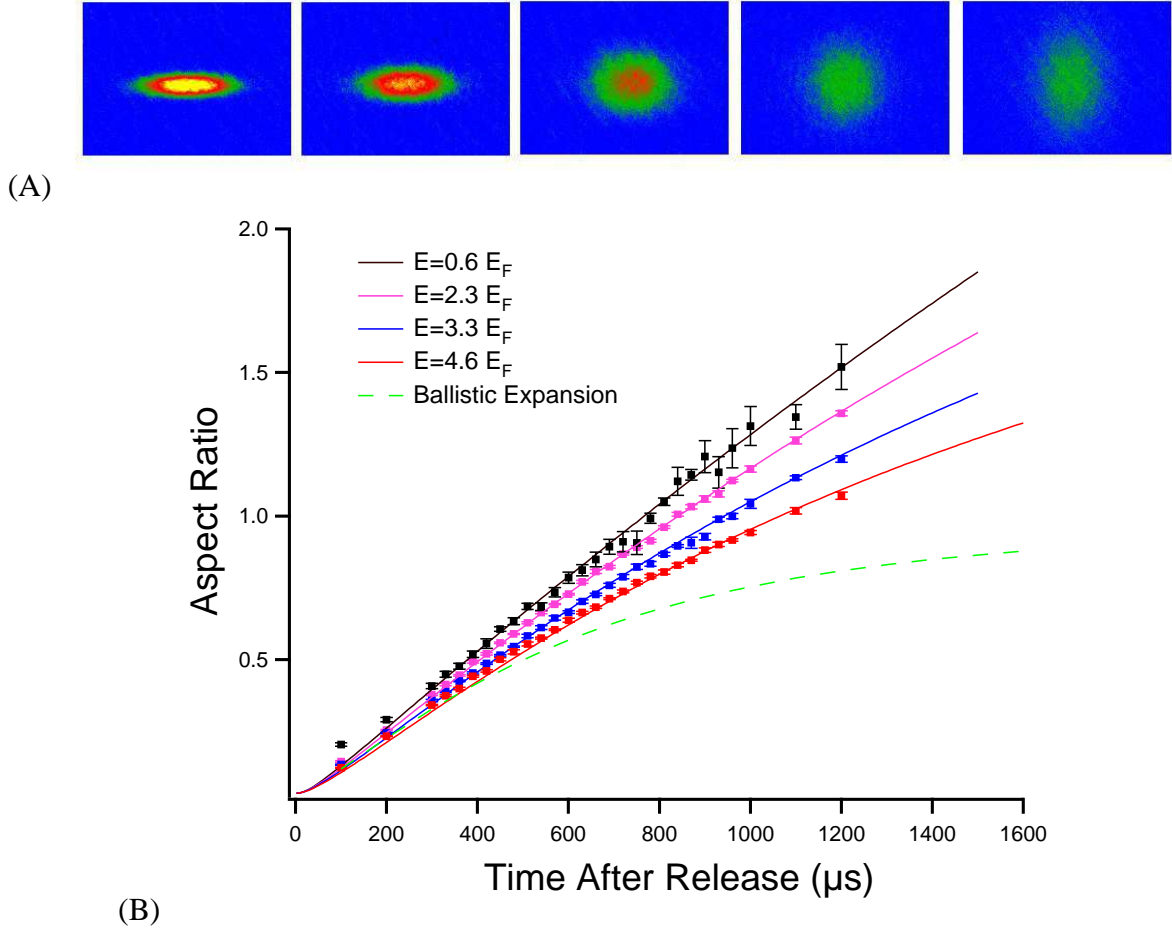


Figure 1: Anisotropic expansion. (A) Cloud absorption images for 0.2, 0.3, 0.6, 0.9, 1.2 ms expansion time, $E = 2.3 E_F$; (B) Aspect ratio versus time. The expansion rate decreases at higher energy as the viscosity increases. Solid curves: Hydrodynamic theory with the viscosity as the fit parameter. Error bars denote statistical fluctuations in the aspect ratio.

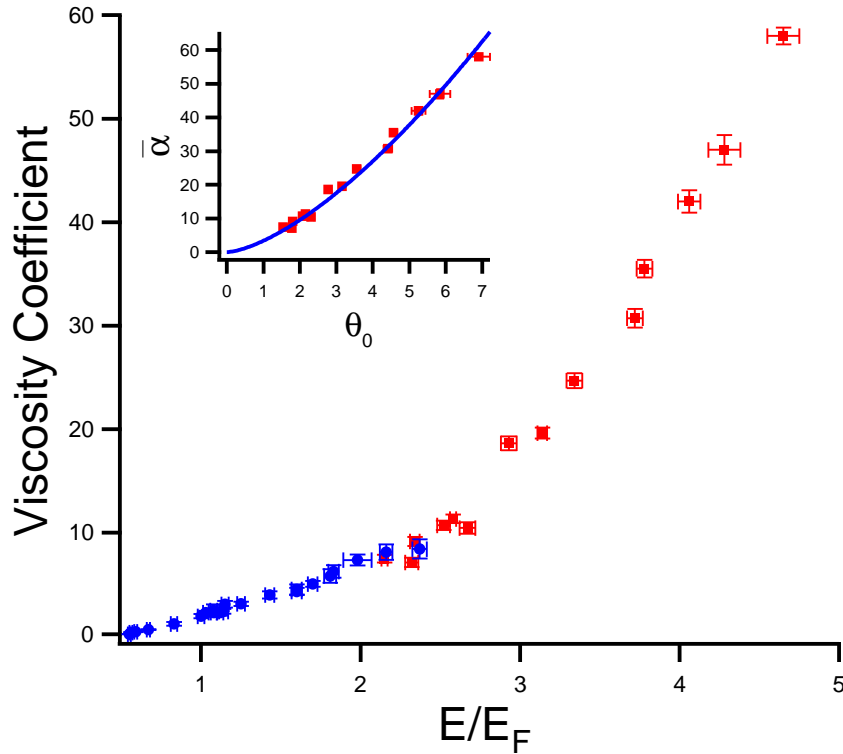


Figure 2: Trap averaged viscosity coefficient $\bar{\alpha} = \int d^3\mathbf{x} \eta / (\hbar N)$ versus initial energy per atom. Blue circles: Breathing mode measurements; Red squares: Anisotropic expansion measurements. Bars denote statistical error arising from the uncertainty in E and the cloud dimensions. Inset: $\bar{\alpha}$ versus reduced temperature θ_0 at the trap center prior to release of the cloud. The blue curve shows the fit $\alpha_0 = \alpha_{3/2} \theta_0^{3/2}$, demonstrating the predicted universal high temperature scaling. Bars denote statistical error arising from the uncertainty in θ_0 and $\bar{\alpha}$. A 3% systematic uncertainty in E_F and 7% in θ_0 arises from the systematic uncertainty in the absolute atom number (20).

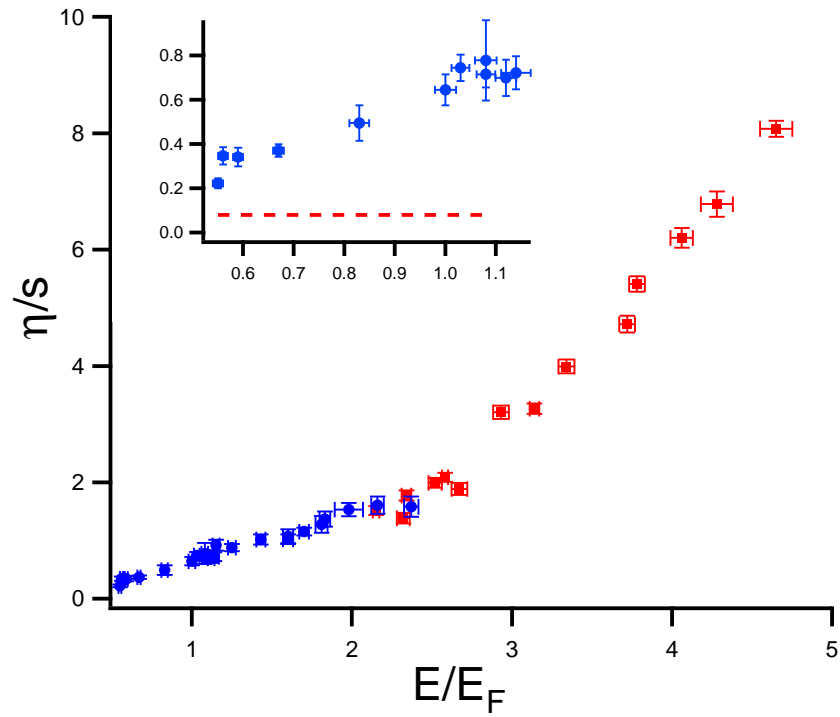


Figure 3: Estimated ratio of the shear viscosity to the entropy density. Blue circles: Breathing mode measurements; Red squares: Anisotropic expansion measurements; Inset: Red dashed line denotes the string theory limit. Bars denote statistical error arising from the uncertainty in E , $\bar{\alpha}$, and S (20).